

An Error Analysis of the Phased Array Antenna Pointing Algorithm for STARS Flight Demonstration #2

Michael P. Carney
Northwestern University
McCormick School of Engineering and Applied Science
C/O Cooperative Educational Office
2145 Sheridan Rd.
Evanston, IL 60208-3122
m-carney@northwestern.edu

James C. Simpson
NASA YA-D7
Kennedy Space Center, FL 32899
James.C.Simpson@nasa.gov

Introduction:

STARS is a multicenter NASA project to determine the feasibility of using space-based assets, such as the Tracking and Data Relay Satellite System (TDRSS) and Global Positioning System (GPS), to increase flexibility (e.g. increase the number of possible launch locations and manage simultaneous operations) and to reduce operational costs by decreasing the need for ground-based range assets and infrastructure. The STARS project includes two major systems: the Range Safety and Range User systems. The latter system uses broadband communications (125 kbps to 500 kbps) for voice, video, and vehicle/payload data. Flight Demonstration #1 revealed the need to increase the data rate of the Range User system. During Flight Demo #2, a Ku-band antenna will generate a higher data rate and will be designed with an embedded pointing algorithm to guarantee that the antenna is pointed directly at TDRS. This algorithm will utilize the onboard position and attitude data to point the antenna to TDRS within a 2-degree full-angle beamwidth. This report investigates how errors in aircraft position and attitude, along with errors in satellite position, propagate into the overall pointing vector.

Explanation of Variables between the Aircraft and TDRS:

The antenna on the aircraft must have a direct line-of-sight to TDRS, which is represented by the green arrow in figure 1. The vector is defined by azimuth (α) and elevation (ϵ) angles in the antenna platform coordinate system. The antenna's actual pointing vector, represented by the blue arrow and α' and ϵ' , might differ from the desired vector pointing to TDRS. The δ angle is the total difference between the TDRS and antenna directions. This angle must have less than a 2 degree full-angle beamwidth in order for the aircraft's antenna to view TDRS.

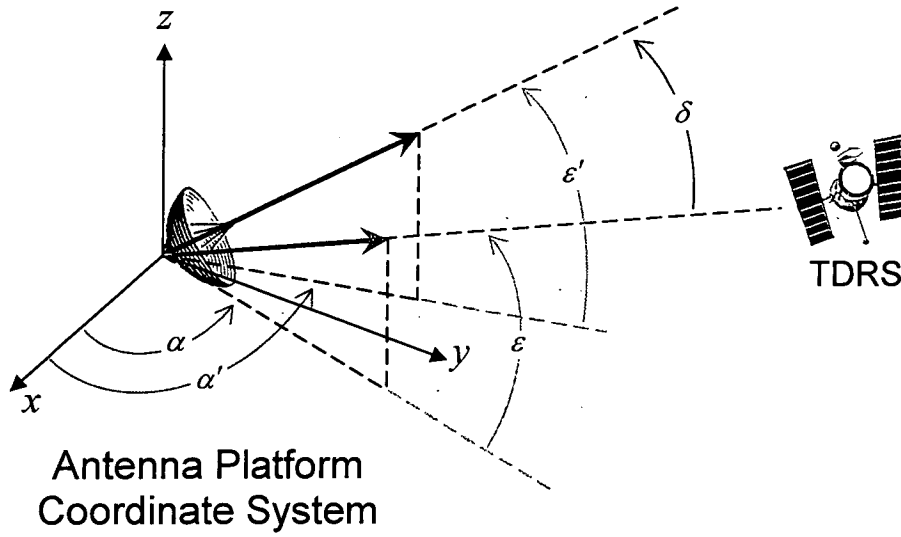


Figure 1. Antenna and TDRS Pointing Vectors

Coordinate Transformations:

TDRSS is nearly geostationary, in a low-inclination orbit with known position represented as latitude, longitude, and altitude. The aircraft's position is represented in the Earth-Centered Earth-fixed (ECEF) coordinate system and its attitude represented as heading, pitch, and roll. The ECEF coordinate system has three axes labeled e, f, and g. The g-axis points from the center of the earth to the north pole (along the axis of rotation); the e-axis points from the center of the earth to the equator at the prime meridian; and the f-axis is derived from the e- and g-axes to be orthogonal, pointing into the Indian Ocean at the equator.

The Dennis.c method is used to convert the TDRSS position from latitude, longitude, and altitude into ECEF coordinates. This method first defines r_{efg} as the radius vector to TDRS in the ECEF system. The latitude and longitude of TDRS (ϕ_T and λ_T) are known, along with the distance from TDRS to Earth center for geosynchronous range (R_T), which can be calculated using Kepler's Third Law.

$$\mathbf{r}_{efg} = \begin{pmatrix} R_T \cos \phi_T \cos \lambda_T \\ R_T \cos \phi_T \sin \lambda_T \\ R_T \sin \phi_T \end{pmatrix}$$

These three values represent the E, F, and G coordinates of TDRSS, respectively. The aircraft's E, F, and G coordinates were included in the flight data for flight 6. The

aircraft's ECEF position vector is subtracted from the TDRS position vector to form the first pointing vector P .

This vector must now be transformed from the ECEF coordinate system to the Local Horizontal Coordinate System. This coordinate system is also called the earth-fixed axis or the geographic coordinate system. One axis points to the north, one to the east, and one axis is either up or down. For this application we will be using the north-east-up method (NEU). The local horizontal system is related to the ECEF system through latitude, longitude, and altitude. The specific method for the NEU transformation is provided below, and results in the second pointing vector, P' :

$$\begin{aligned} P' &= \Phi \cdot P \\ &= (\Phi_{-z} \cdot \Phi_{\phi} \cdot \Phi_{\lambda} \cdot \Phi_{\pi/2}) \cdot P \\ \Phi &= \begin{pmatrix} -\cos \lambda \sin \phi & -\sin \lambda \sin \phi & \cos \phi \\ -\sin \lambda & \cos \lambda & 0 \\ \cos \lambda \cos \phi & \sin \lambda \cos \phi & \sin \phi \end{pmatrix} \end{aligned}$$

Once the pointing vector is in the Local Horizontal Coordinate System, the corresponding matrix must be rotated about the NEU coordinates in order to take into account the attitude of the aircraft. After the rotation, the new coordinates are in the Body-Axis coordinate system, also known as the body platform coordinate system. It is a right-handed system with x-axis forward, y-axis to the right, and z-axis pointed down. This coordinate system is related to the local horizontal system through the heading, pitch, and roll angles of the aircraft.

The specific method for the transformation is included below, and results in the third pointing vector, P'' . The order of rotation is of particular importance:

$$\begin{aligned} P'' &= \Gamma \cdot P' = (\Gamma_R \cdot \Gamma_P \cdot \Gamma_H) \cdot P' \\ \Gamma_H &= \begin{pmatrix} \cos H & \sin H & 0 \\ -\sin H & \cos H & 0 \\ 0 & 0 & 1 \end{pmatrix} \quad \Gamma_P = \begin{pmatrix} \cos P & 0 & \sin P \\ 0 & 1 & 0 \\ -\sin P & 0 & \cos P \end{pmatrix} \quad \Gamma_R = \begin{pmatrix} 1 & 0 & 0 \\ 0 & \cos R & -\sin R \\ 0 & \sin R & \cos R \end{pmatrix} \\ \Gamma &= \begin{pmatrix} \cos H \cos P & \cos P \sin H & \sin P \\ -\cos R \sin H + \cos H \sin P \sin R & \cos H \cos R + \sin H \sin P \sin R & -\cos P \sin R \\ -\cos H \cos R \sin P - \sin H \sin R & -\cos R \sin H \sin P + \cos H \sin R & \cos P \cos R \end{pmatrix} \end{aligned}$$

The final azimuth and elevation angles can be derived from the X, Y, and Z components of the P'' vector.

$$\text{Azimuth: } \alpha = \tan^{-1} \left(\frac{P_Y''}{P_X''} \right)$$

$$\text{Elevation: } \varepsilon = \tan^{-1} \left(\frac{P_Z''}{\sqrt{(P_X'')^2 + (P_Y'')^2}} \right)$$

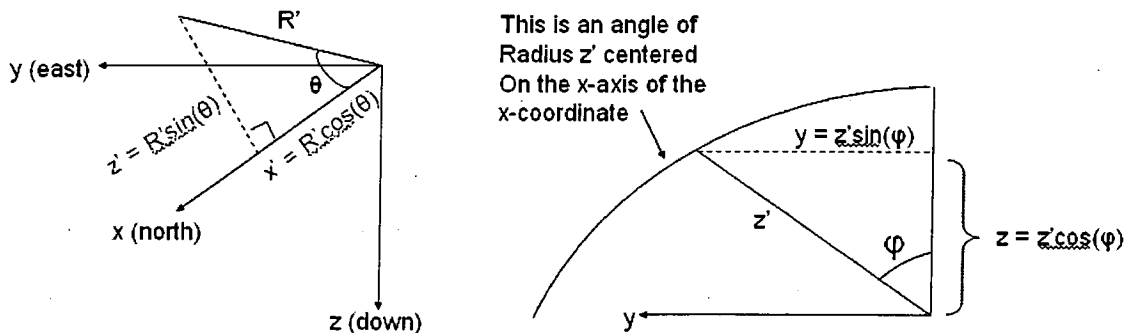
The following section will explain how these values were found to be accurate.

Comparing the Azimuth and Elevation Results with Phi and Theta Aircraft Data:

To ensure the validity of the series of transformations and rotations performed in the previous section, the equations were checked using actual data from Flight Demonstration #1. The data included pointing information in another coordinate system from CLASS, and this data was compared to the data derived in the previous section. The phi and theta data used in the system from CLASS are defined identically to the STARS Flight Demo #1 Report. Specifically:

- theta = 0°, phi = any value is the nose of the F-15
- theta = 180°, phi = any value is the tail of the F-15
- theta = 90°, phi = 0° is straight up
- theta = 90°, phi = 90° is out the starboard wing
- theta = 90°, phi = 180° is straight down
- theta = 90°, phi = 270° is out the port wing

The NED coordinate system was used initially to define phi and theta. The phi and theta coordinates from the flight data were used to convert to azimuth and elevation using the following:



Additionally,

$$x = R' \cos(\theta)$$

$$z' = R' \sin(\theta)$$

$$y = z' \sin(\phi) = R' \sin(\theta) \sin(\phi)$$

$$z = z' \cos(\phi) = R' \sin(\theta) \cos(\phi)$$

The final azimuth and elevation calculations can then be derived:

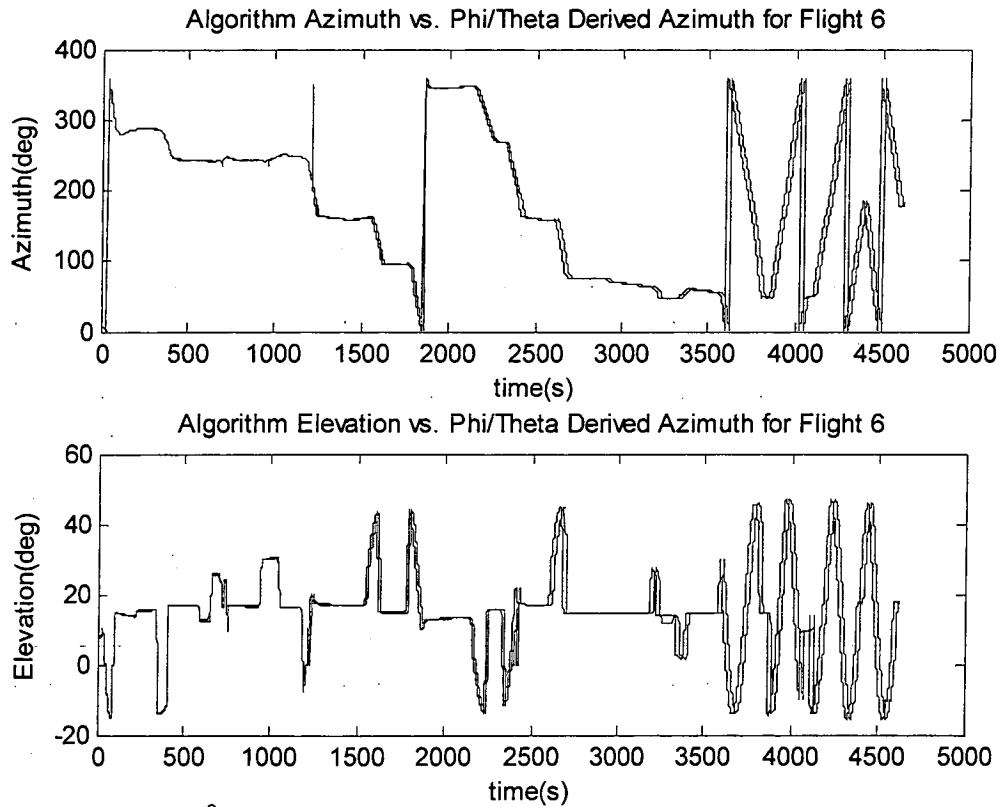
$$\tan az = \frac{y}{x} = \frac{R' \sin(\theta) \sin(\varphi)}{R' \cos(\theta)} = \frac{\sin(\theta) \sin(\varphi)}{\cos(\theta)}$$

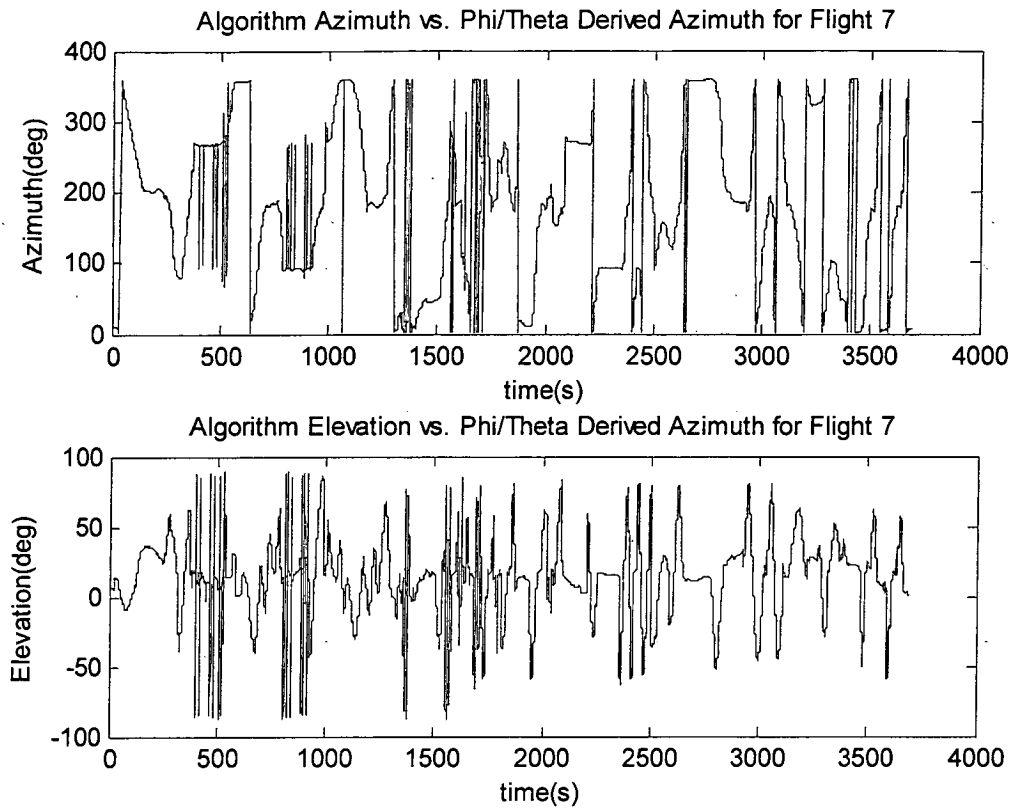
$$az = \tan^{-1} \left(\frac{\sin(\theta) \sin(\varphi)}{\cos(\theta)} \right)$$

$$\tan el = \frac{z}{\sqrt{x^2 + y^2}} = \frac{R' \sin(\theta) \cos(\varphi)}{\sqrt{R'^2 \cos^2(\theta) + R'^2 \sin^2(\theta) \sin^2(\varphi)}}$$

$$el = \tan^{-1} \left(\frac{\sin(\theta) \cos(\varphi)}{\sqrt{\cos^2(\theta) + \sin^2(\theta) \sin^2(\varphi)}} \right)$$

The two separate calculations for azimuth and elevation were then plotted against each other:





Errors Added into the Algorithm:

After confirming the azimuth and elevation values, errors were added into the position and attitude of the aircraft at each time increment. The “perturbed” values of position and attitude were subtracted from the original values to form a new “perturbed” value of azimuth and elevation. In addition, the overall angle between the antenna’s pointing vector and the TDRS pointing vector, called delta, was calculated using the spherical law of cosines, or:

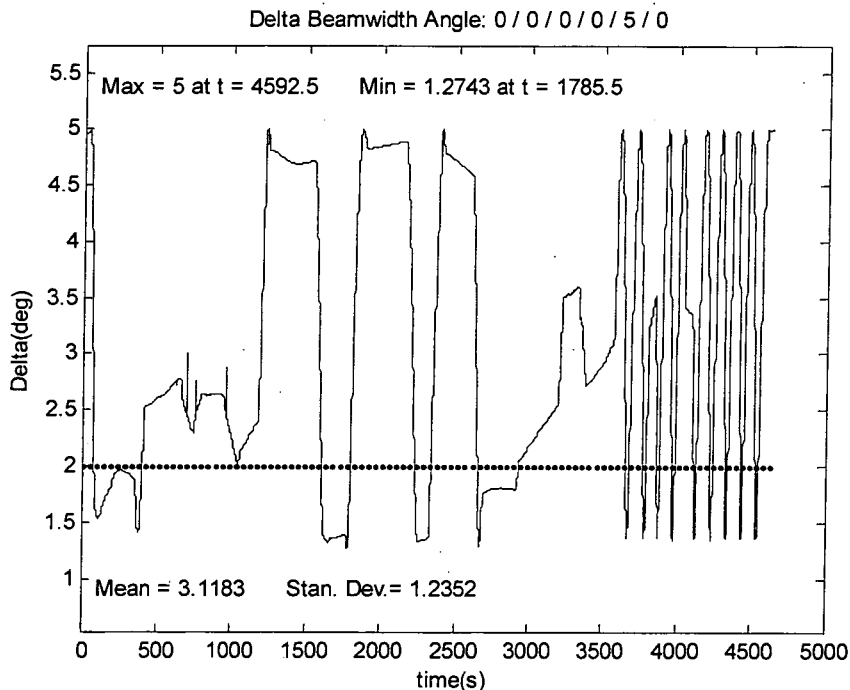
$$\begin{aligned}\hat{e}_{TDRS} \cdot \hat{e}_{ANT} &= (1)(1) \cos \delta \\ &= \sin \varepsilon \sin \varepsilon' + \cos \varepsilon \cos \varepsilon' \cos(\alpha - \alpha')\end{aligned}$$

The variables in this equation have been defined previously. Since all variables have known values, the delta angle can be found simply using trigonometry. The azimuth and elevation delta values were then plotted against time to reveal the effects of the errors.

Results:

Aircraft position errors seemed to have a much reduced effect on the data than did changes in aircraft attitude or TDRS position. A 1-degree change in heading, pitch, or roll created significant differences in azimuth and elevation delta values, but even a 10,000 meter change in position had little effect. Change in TDRS position had an even greater effect, with a 0.05 degree change in latitude or longitude pushing the overall delta

value beyond the 2 degree full-angle beamwidth (see plot below). The numbers next to the title of the plot signify the error of terms in the following order: x-position / y-position / z-position / heading-angle / pitch-angle / roll-angle. Also included are the minimum and maximum delta and the times at which they occurred, the mean delta, and the standard deviation of the delta. The plot below includes a dotted line at 2-degrees to distinguish between valid and invalid data. It was taken from flight 6 data; flight 7 data was taken at a higher frequency and had a much greater change in the magnitude of the delta values.



Summary of Results:

Flight	# of Trials	Quantity Perturbed	Size of Perturbation	Elevation Error (°)	Azimuth Error (°)	Delta (°)
6	10	E (aircraft)	-10km → 10km	-0.1 → 0.1	-0.1 → 0.1	0.1
6	10	F (aircraft)	-10km → 10km	-0.05 → 0.05	-0.08 → 0.08	0.06
6	10	G (aircraft)	-10km → 10km	-0.05 → 0.05	-0.05 → 0.05	0.05
6	14	H (heading)	-20° → 20°	-10 → 10	-28 → 28	19.2 ± 0.1
6	14	P (pitch)	-20° → 20°	-20 → 20	-12 → 12	5.1 → 20
6	14	R (roll)	-20° → 20°	-20 → 20	-17 → 17	2 → 20
6	8	TDRS Lat.	-2° → 2°	-2 → 2	-2.5 → 2.5	2.1
6	8	TDRS Long.	-2° → 2°	-2 → 2	-2.5 → 2.5	2.1
7	10	E (aircraft)	-10km → 10km	-0.1 → 0.1	-8.9 → 7.6	0.1
7	10	F (aircraft)	-10km → 10km	-0.06 → 0.06	-3.9 → 3.4	0.06
7	10	G (aircraft)	-10km → 10km	-0.05 → 0.05	-3.0 → 3.3	0.05
7	14	H (heading)	-20° → 20°	-19.2 → 19.2	-175 → 180	19.2 ± 0.1
7	14	P (pitch)	-20° → 20°	-20 → 20	-171 → 169	5.33 → 20

7	14	R (roll)	$-20^{\circ} \rightarrow 20^{\circ}$	$-20 \rightarrow 20$	$-180 \rightarrow 180$	$0.01 \rightarrow 20$
7	2	TDRS Lat.	$-1^{\circ} \rightarrow 1^{\circ}$	$-2.1 \rightarrow 2.1$	most within $\pm 10^{\circ}$, some up to $\pm 50^{\circ}$	2.1
7	2	TDRS Long.	$-1^{\circ} \rightarrow 1^{\circ}$	$-2.1 \rightarrow 2.1$	most within $\pm 10^{\circ}$, some up to $\pm 50^{\circ}$	2.1